

1 **Replication-uncoupled histone deposition during adenovirus DNA replication**

2

3 **Tetsuro Komatsu and Kyosuke Nagata***

4

5 Department of Infection Biology, Faculty of Medicine and Graduate School of
6 Comprehensive Human Sciences, University of Tsukuba, Tsukuba 305-8575, Japan

7

8 *Corresponding author. Department of Infection Biology, Faculty of Medicine and
9 Graduate School of Comprehensive Human Sciences, University of Tsukuba, 1-1-1

10 Tennodai, Tsukuba 305-8575, Japan. Phone and fax: (81) 298-53-3233. E-mail:

11 knagata@md.tsukuba.ac.jp.

12

13 Running title: DBP and histone H3.3 in adenovirus DNA replication

14 ABSTRACT: 203 words

15 TEXT: 5255 words

16

17 **ABSTRACT**

18 In infected cells, the chromatin structure of the adenovirus genome DNA
19 plays critical roles in its genome functions. Previously, we have reported that in early
20 phases of infection, incoming viral DNA is associated with both viral core protein VII
21 and cellular histones. Here we show that in late phases of infection, newly synthesized
22 viral DNA is also associated with histones. We also found that knockdown of CAF-1,
23 a histone chaperone that functions in replication-coupled deposition of histones, does
24 not affect the level of histone H3 bound on viral chromatin, although CAF-1 is
25 accumulated at viral DNA replication foci together with PCNA. Chromatin
26 immunoprecipitation assays using epitope-tagged histone H3 demonstrated that histone
27 variant H3.3, which is deposited onto the cellular genome in a replication-independent
28 manner, is selectively associated with both incoming and newly synthesized viral DNAs.
29 Microscopic analyses indicated that histones but not USF1, a transcription factor that
30 regulates viral late gene expression, are excluded from viral DNA replication foci and
31 this is achieved by oligomerization of DBP. Taken together, these results suggest that
32 the histone deposition onto newly synthesized viral DNA is most likely uncoupled with
33 viral DNA replication, and a possible role of DBP oligomerization in this
34 replication-uncoupled histone deposition is discussed.

35

36 INTRODUCTION

37 In the cell nucleus, the genomic DNA is not naked, but forms chromatin
38 structure with chromatin proteins. The fundamental unit of the chromatin structure is a
39 nucleosome, which consists of histone octamer (two copies each of histone H2A, H2B,
40 H3, and H4) and DNA wrapping around the octamer. Deposition of histones and/or
41 remodeling of nucleosome arrays are critical processes for the expression of genome
42 functions (2), since nucleosome packaging could be barrier for *trans*-acting factors to
43 access their cognate sites on DNA. Thus, the nucleosome structure must be strictly
44 and dynamically regulated in connection with several events on chromatin, such as
45 transcription, DNA replication, and DNA repair.

46 Currently, it is known that histone deposition is carried out mainly by two
47 fashions, DNA replication-dependent and independent ones, and a role of histone
48 variants in these deposition pathways has been elucidated (14). In mammalian somatic
49 cells, there are three major histone H3 variants, H3.1, H3.2, and H3.3, and they have
50 only slight differences in amino acid (aa) sequences (16). The canonical histone H3,
51 histone H3.1 and highly related variant H3.2 (which differs only 1 aa from H3.1) are
52 expressed exclusively during S phase, while the expression of the variant H3.3 that
53 differs 4 and 5 aa from H3.2 and H3.1, respectively, is observed throughout cell cycle.
54 Thus, this variant is called “replication-independent” one (11). Tagami *et al.*
55 demonstrated that the canonical histone H3 (H3.1) interacts with histone chaperone
56 CAF-1 complex and is deposited onto DNA in a replication-dependent manner, while
57 HIRA specifically binds to and deposits histone variant H3.3 onto DNA independently

58 of DNA synthesis (43). CAF-1 is composed of three subunits, p150, p60, and p48, and
59 associated with the cellular DNA replication machinery through the interaction with
60 PCNA, a sliding clamp for DNA polymerases, allowing DNA replication-coupled
61 deposition of histones (40, 41, 50). On the other hand, HIRA was identified as a DNA
62 synthesis-independent histone chaperone by *cell-free* systems using *Xenopus* egg
63 extracts (32), and histone variant H3.3 is shown to mark transcriptional active genomic
64 regions (1). Furthermore, additional H3.3-specific chaperones are recently identified.
65 Daxx is one of components of PML nuclear bodies and reported to deposit histone H3.3
66 onto the specific genomic regions such as telomeres and pericentric heterochromatin,
67 together with an ATP-dependent chromatin remodeler, ATRX (10, 21). It is also
68 reported that in *Drosophila* cells, DEK is a coactivator of a nuclear receptor and
69 functions as an H3.3-specific chaperone (37). Thus, the mechanistic evidences for
70 histone deposition are accumulating, in the case of cellular chromatin.

71 The regulatory events for chromatin structure are not limited to the cellular
72 genome, as some viruses also have chromatin and/or chromatin-like structures with
73 their own genomes. The adenovirus (Ad) genome is a linear double-stranded DNA
74 (dsDNA) of ~36000 bp in length. In the virion, the Ad genome forms chromatin-like
75 structure with viral basic core proteins, as it is revealed by electron microscopic
76 analyses that viral core protein-DNA complexes purified from the virion show
77 “beads-on-a-string” structure (49). Among core proteins, protein VII is a major DNA
78 binding protein that can introduce superhelical turns into DNA as do cellular histones
79 (4), and remains associated with viral DNA after the entry of the nucleus (7, 17).

80 When viral DNA-core protein complexes purified from the virion are used as a template
81 for *cell-free* DNA replication/transcription systems, the reactions occur at a much lower
82 level, compared with the case of naked DNA, indicating that viral chromatin-like
83 structure must be remodeled to execute its genome functions (22, 23). Previously, we
84 have identified host cell-derived remodeling factors for Ad chromatin with biochemical
85 analyses (19, 22, 24, 26) and demonstrated that TAF-I, one of these host factors, plays
86 an important role in the regulation of viral early gene expression in infected cells
87 through the interaction with protein VII (15, 17, 18, 20, 27). Thus, it is indicated that
88 remodeling of Ad chromatin is a crucial process for its genome functions (13), as is the
89 case for the cellular genome. In addition, recently we have reported using chromatin
90 immunoprecipitation (ChIP) assays that in early phases of infection, cellular histones
91 are incorporated into viral DNA-protein VII complexes and histone modification occurs
92 depending upon transcription states on viral chromatin, suggesting that cellular histones
93 could be functional components of viral chromatin in infected cells (20).

94 As described above, although viral chromatin structure and its regulation in
95 early phases of infection are being clarified, it is quite unclear how viral chromatin
96 structure is regulated in late phases of infection. In particular, since the expression of
97 viral late genes is largely dependent on its own DNA replication (45), the regulation of
98 the chromatin structure during viral DNA replication could be a key step. Therefore,
99 in this study we sought to elucidate the regulatory mechanism how the chromatin
100 structure is formed on newly synthesized viral DNA through viral DNA replication, in
101 particular with respect to the histone deposition. We found that after the onset of viral

102 DNA replication, cellular histones are also incorporated into viral chromatin. We also
103 found that although CAF-1 is accumulated at the site of viral DNA replication, this
104 factor seems not to be involved in the histone deposition during viral DNA replication,
105 since knockdown of CAF-1 did not affect the binding level of histone H3 on viral
106 chromatin and histone variant H3.3, which is deposited onto DNA in a DNA
107 synthesis-independent manner, is specifically deposited onto viral DNA even after the
108 onset of viral DNA replication. Microscopic analyses suggest that histones but not
109 USF1, a transcription factor which is shown to bind to and regulate transcription from
110 viral major late promoter (MLP) (46), are excluded from the site of viral DNA
111 replication, possibly by oligomerization of Ad single-stranded DNA (ssDNA) binding
112 protein (DBP), one of viral DNA replication factors. Based on these results, we would
113 propose a model that unlike cellular chromatin, the histone deposition onto the newly
114 synthesized viral DNA is not coupled with viral DNA replication. A feasible role of
115 this uncoupled deposition mechanism mediated by DBP oligomerization on Ad genome
116 functions is discussed.
117

118 **MATERIALS AND METHODS**

119 **Cells and viruses.**

120 Maintenance of HeLa cells, and purification and infection of human
121 adenovirus type 5 (HAdV5) were carried out essentially as described previously (18,
122 20). Hydroxyurea (HU) was added at the final concentration of 2 mM right after
123 infection when DNA replication was to be blocked. HeLa cells stably expressing
124 EGFP-tagged histone H3.2 and H3.3 [a kind gift from Dr. M. Okuwaki (University of
125 Tsukuba)] were also maintained as described above. Transfection of expression
126 plasmids was performed using GeneJuice (Novagen) according to the manufacturer's
127 protocol.

128

129 **Antibodies.**

130 Antibodies used in this study are as follows: rabbit anti-histone H3 (catalog
131 no. ab1791; abcam), rabbit anti-histone H4 (catalog no. 04-858; Millipore), rabbit
132 anti-histone H2A (catalog no. ab18255; abcam), mouse anti-HIRA (catalog no. 04-1488;
133 Millipore), mouse anti-FLAG M2 (catalog no. F3165; Sigma), rat anti-HA (3F10;
134 Roche), and mouse anti- β -actin (Sigma) antibodies. Rabbit anti-histone H2A-H2B,
135 mouse anti-CAF-1 p150, and mouse anti-DBP antibodies were kindly provided by Dr.
136 M. Okuwaki (University of Tsukuba), Dr. A. Verreault (University of Montreal), and Dr.
137 W. C. Russel, respectively. Rat anti-protein VII antibody was described elsewhere
138 (17).

139

140 **Vector construction.**

141 To construct the expression vectors for USF1, full-length DBP, and its deletion
142 mutant (DBP Δ C, which lacks the C-terminal 17 aa), cDNA fragments of USF1, DBP,
143 and DBP Δ C were amplified by PCR, digested with BamHI and EcoRI, and cloned
144 in-frame into pCHA vector containing a hemagglutinin (HA) epitope tag and the
145 puromycin-resistance gene [pCHA-puro vector, kindly provided from K. Kajitani
146 (University of Tsukuba)]. The resulting vectors are designated pCHA-puro-USF1,
147 pCHA-puro-DBP, and pCHA-puro-DBP Δ C, respectively. Similarly, for the
148 expression vector of PCNA, amplified cDNA fragment was digested with BamHI and
149 cloned into pCHA-puro vector digested with BamHI and EcoRV (pCHA-puro-PCNA).

150 The primers used here were as follows:

151 5'-GTTTAGGATCCCATATGAAGGGGCAGCAG-3' and

152 5'-GGGCCGAATTCTTAGTTGCTGTCATTCTTG-3' for USF1 cDNA,

153 5'-AAAGGATCCATGGCCAGTCGGG-3' and

154 5'-GCGGAATTCTTAAAAATCAAAGGGGTTCTG-3' for DBP cDNA,

155 5'-AAAGGATCCATGGCCAGTCGGG-3' and

156 5'-CCCGAATTCTTAGTTGCGATACTGG-3' for DBP Δ C cDNA, and

157 5'-AAAGGATCCATGTTCGAGGCGC-3' and

158 5'-ATCGTCGACCTAAGATCCTTCTTC-3' for PCNA cDNA.

159 For preparation of cells stably expressing HA-PCNA, HeLa cells were transfected
160 with pCHA-puro-PCNA and cultured in the presence of 2 μ g/mL puromycin for 2
161 weeks.

162 For construction of the expression vector of histone H3.1, cDNA fragment of
163 histone H3.1 was amplified by PCR, digested with NcoI, and cloned into pBS-FLAG
164 vector (pBS-H3.1-FLAG). Then, the DNA fragment containing cDNA of H3.1 and
165 the C-terminal FLAG tag was obtained from pBS-H3.1-FLAG by digestion with
166 BamHI and EcoRI, and cloned into pcDNA3 vector (pcDNA3-H3.1-FLAG). The
167 primers used here were as follows: 5'-AAAACCATGGCGCGTACTAAGCAG-3' and
168 5'-TTATTCCATGGCCGCCCTCTCCCCA-3'.

169 The expression vectors for FLAG-tagged histone H3.2 and H3.3
170 (pcDNA3-H3.2-FLAG and pcDNA3-H3.3-FLAG) and HA-tagged DEK (pCHA-DEK)
171 were generously provided by Dr. M. Okuwaki and Dr. S. Saito, respectively (University
172 of Tsukuba).

173

174 **Indirect immunofluorescence assays.**

175 Indirect immunofluorescence (IF) assays were carried out essentially as
176 previously described (18). Localization of the protein was visualized with the
177 secondary antibodies (anti-mouse IgG conjugated with AlexaFluor 488, anti-mouse IgG
178 conjugated with AlexaFluor 568, and anti-rabbit IgG conjugated with AlexaFluor 568;
179 Invitrogen). DNA was visualized by staining with TO-PRO-3 iodide (Invitrogen).
180 Labeled cells were observed with confocal laser scanning microscopy (LSM5 Exciter;
181 Carl Zeiss) using argon laser (488 nm) and He/Ne laser (546 and 633 nm) lines.

182

183 **ChIP, RT-PCR, siRNA-mediated knockdown, and western blot assays.**

184 These experiments were carried out essentially as described previously (20).
185 siRNA targeted for CAF-1 p150 was commercially purchased (Stealth siRNA;
186 Invitrogen). Primers for *CAF-1 p150* mRNA are as follows:
187 5'-GGAGCAGGACAGTTGGAGTG-3' and 5'-GACGAATGGCTGAGTACAGA-3'.
188 Other primers for CHIP and RT-PCR assays were described elsewhere (20). In all the
189 experiments by quantitative PCR (qPCR), mean values with SD were obtained from
190 three independent experiments.
191

192 **RESULTS**

193 **Cellular histones are bound with viral chromatin both in early and late phases of**
194 **infection.**

195 Previously, we reported that in early phases of infection (before the onset of viral
196 DNA replication), viral chromatin is composed of both viral core protein VII and
197 cellular histones and this “chimeric” chromatin functions as template for transcription
198 (20). To examine whether histones are also bound with viral chromatin after the onset
199 of viral DNA replication, we performed ChIP assays using antibodies against histones
200 and protein VII (Fig. 1). The viral DNA replication starts around 8 hpi (hours post
201 infection) in our condition (17, 20). In order to reveal the viral chromatin state
202 during/right after viral DNA replication, HeLa cells infected at an MOI (multiplicity of
203 infection) of 100 were harvested at 6 and 12 hpi for ChIP assays. We chose five
204 regions for ChIP assays, four viral genome regions (E1A pro, MLP, Hexon, E4 pro, Fig.
205 1A) and one cellular genomic region (ribosomal RNA gene, rDNA) as a control (20).
206 In this condition, the amount of viral DNA was increased by ~20 fold through viral
207 DNA replication (Fig. 1B). At 6 hpi, all core histones are bound with viral chromatin,
208 but at the low binding level compared with cellular chromatin (Fig. 1C, histone H3, H4,
209 and H2A-H2B). This was in good agreement with our previous observation (20). At
210 12 hpi, core histones were also found to be associated with viral chromatin. The
211 binding level of histones on viral chromatin at 12 hpi was more than those at 6 hpi, but
212 slightly less than those on cellular chromatin. This is consistent with the previous
213 report of electron microscopic analyses showing that viral genome DNA purified from

214 infected cells at late phases of infection has the nucleosome-like particles, which are
215 less dense compared with cellular nucleosome arrays (3). In contrast, the binding level
216 of protein VII was drastically decreased after the onset of viral DNA replication (Fig.
217 1C, protein VII), suggesting that newly synthesized viral DNA is mainly associated with
218 cellular histones. We do not exclude the possibility that protein VII remains associated
219 with small population of viral chromatin because the binding level of protein VII on
220 viral chromatin was still higher than that on cellular chromatin even at 12 hpi. The
221 ratio among core histones bound on viral chromatin was almost the same as that on
222 cellular chromatin both at 6 (data not shown, 20) and 12 hpi (Fig. 1D), indicating that
223 viral chromatin contains the canonical nucleosome structure.

224

225 **CAF-1 and PCNA are not involved in the histone deposition onto newly**
226 **synthesized viral DNA.**

227 It is known that during DNA replication of the cellular genome and some DNA
228 virus genomes, histones are deposited by CAF-1, a replication-dependent histone
229 chaperone (41, 43). CAF-1 is associated with the DNA replication machinery through
230 the interaction with PCNA, thereby enabling replication-coupled deposition of histone
231 H3-H4 complexes (40). Thus, it is worthwhile to examine whether CAF-1 and PCNA
232 are also involved in the histone deposition onto newly synthesized Ad DNA, although
233 there is no definitive evidence that those two are involved in the Ad DNA replication.
234 To test this, we first performed IF assays using cells stably expressing HA-tagged
235 PCNA (HA-PCNA) to examine the relationship among viral DNA replication, PCNA,

236 and CAF-1 (Fig. 2A). Using antibody against DBP, Ad ssDNA binding protein
237 involved in viral DNA replication, the place for viral DNA replication designated “viral
238 DNA replication foci” (hereafter referred to as “VDRF”) can be visualized (31). HeLa
239 cells or cells stably HA-PCNA were infected at an MOI of 50, and at 18 hpi subjected to
240 IF assays using anti-DBP and anti-HA antibodies. In mock-infected cells, HA-PCNA
241 was localized throughout the nucleus and shows the punctate localization in some cell
242 population, as reported previously (29). At 18 hpi, VDRF was observed as a
243 donut-like signal using anti-DBP antibody, and we found that HA-PCNA showing
244 punctate localization was accumulated inside VDRF. We also observed the similar
245 localization pattern of CAF-1 inside VDRF (see below in Fig. 4A). These results
246 suggest that PCNA and CAF-1 are recruited together into the site of viral DNA
247 replication.

248 Next, to investigate a role of CAF-1 in the histone deposition onto viral DNA,
249 siRNA-mediated knockdown of CAF-1 p150, a largest subunit of CAF-1 complex, was
250 carried out (Fig. 2B, C, and D). HeLa cells were treated with control siRNA (siCont)
251 or siRNA for CAF-1 p150 (siCAF-1), infected with HAdV5 at an MOI of 100, and
252 harvested at 6 and 12 hpi. First, we examined the knockdown efficiency of CAF-1
253 p150 by RT-qPCR assays (Fig. 2B). The mRNA level of CAF-1 p150 in
254 siRNA-treated cells was about 20% of those in control cells, although at 12 hpi the level
255 was slightly increased possibly due to S-phase like environment induced by Ad
256 infection (30). In contrast, the mRNA level of GAPDH was almost unaffected by
257 siRNA treatment and Ad infection. In this condition, the binding level of histone H3

258 on viral chromatin was examined by ChIP assays (Fig. 2C). The binding level of H3
259 on viral chromatin was not decreased by CAF-1 knockdown, and rather slightly
260 increased (but not statistically significant) at 12 hpi (Fig. 2C, E1A pro and MLP). It is
261 noted that the binding level of H3 on cellular chromatin was also unaffected by CAF-1
262 knockdown (Fig. 2C, rDNA, see Discussion). In addition, we could not observe any
263 effect of CAF-1 knockdown on viral DNA replication levels (Fig. 2D). Taken together,
264 these results suggest that it is not likely that CAF-1 is involved in the histone deposition
265 onto viral chromatin during viral DNA replication, although CAF-1 is accumulated at
266 VDRF together with PCNA.

267

268 **Replication-independent histone H3.3 is selectively incorporated into viral**
269 **chromatin.**

270 It is known that among histone H3 variants, histone H3.1 and H3.2 are
271 deposited onto DNA by CAF-1 during DNA replication, while H3.3 is deposited
272 independently of DNA replication (11, 14). If CAF-1 is not involved in the histone
273 deposition during viral DNA replication, histone H3.3 rather than H3.1 and H3.2 could
274 be incorporated into newly synthesized viral DNA. Therefore, to examine this
275 possibility, we performed ChIP assays using FLAG-tagged histone H3.2 and H3.3 (Fig.
276 3). HeLa cells were transfected with expression vectors for H3.2 and H3.3 and at 24
277 hpt (hours post transfection) infected at an MOI of 100. We first studied using cells at
278 early phases of infection (before the onset of viral DNA replication) (Fig. 3A).
279 Infected cells were harvested at 2 and 6 hpi, and at 10 hpi in presence of HU to block

280 viral DNA replication (20), and subjected to ChIP assays with anti-FLAG antibody.
281 As shown in Figure 3A, the exclusive binding of H3.3 on viral chromatin was observed
282 at all the regions we tested, with a gradual increment as infection proceeded. This is
283 consistent with the recent report on helper-dependent Ad vector (HdAd) indicating that
284 histone H3.3 are specifically deposited onto HdAd DNA by HIRA, an H3.3-specific
285 histone chaperone (34). Since HdAd alone does not undergo its DNA replication, the
286 chromatin state of HdAd may reflect that of wildtype Ad in early phases of infection (13,
287 34).

288 Next we performed ChIP assays at 12 hpi to examine which H3 variant is
289 deposited onto newly synthesized viral DNA (Fig. 3B). We found that histone H3.3
290 but not H3.2 was associated with viral chromatin at this time point, as observed in early
291 phases of infection. The expression levels of both H3 variants were comparable (Fig.
292 3C), and both variants were associated with cellular chromatin with a similar binding
293 level (Fig. 3A and B, rDNA). These strongly suggest that this result was not due to
294 some technical issues. Further, we obtained the same results by using FLAG-tagged
295 histone H3.1 instead of H3.2 (Fig. 3D and E). Thus, these results suggest that
296 replication-independent histone variant H3.3 is selectively deposited onto not only
297 incoming but also newly synthesized viral DNA in infected cells.

298

299 **Histones but not transcription factor USF1 are excluded from the site of viral DNA**
300 **replication.**

301 To further investigate the histone fluctuation during viral DNA replication, we

302 performed IF analyses using HeLa cells stably expressing EGFP-tagged histone H3.3
303 (Fig. 4A). Cells were infected at an MOI of 50, and at 18 hpi subjected to IF assays
304 using anti-DBP antibody (Fig. 4A, upper panels). VDRF was observed at 18 hpi as
305 described above, and H3.3-EGFP was found to be excluded from VDRF. Similar
306 results were obtained by using cells stably expressing EGFP-tagged histone H3.2 (Fig.
307 4B). This was due to neither exogenous expression nor EGFP tag of H3 variants as we
308 observed the similar exclusion of the endogenous histone using anti-histone H2A
309 antibody (Fig. 4C). This localization pattern was specific for late phases of infection
310 since the localization of EGFP-tagged H3 variants was not changed in early phases of
311 infection (Fig. 4D). We also performed IF analyses using anti-CAF-1 p150 antibody
312 and observed that CAF-1 was accumulated at “histone-less” region, that is, VDRF (Fig.
313 4A, lower panels), as was observed with HA-PCNA (Fig. 2A). In summary, these
314 results indicated that histones are localized reciprocally to VDRF (and CAF-1/PCNA)
315 in late phases of infection.

316 To gain more insights into the accessibility of other nuclear proteins to VDRF,
317 we again performed IF analyses (Fig. 5). First, IF analyses were carried out using
318 antibody against HIRA, an H3.3-specific histone chaperone, and it was observed that
319 the localization of HIRA was not drastically changed in both early and late phases of
320 infection (Fig. 5A). We also performed IF analyses using cells transiently transfected
321 with expression vectors for HA-tagged DEK and USF1 (Fig. 5B and C). DEK is a
322 cellular chromatin protein with potential histone chaperone activity (37), and USF1 is
323 an E-box-binding transcription factor and reported to bind to and regulate transcription

324 from the MLP region (46). HeLa cells were transfected with expression vectors and at
325 24 hpt subjected to western blot analyses (Fig. 5B) or infected at an MOI of 50. At 18
326 hpi, localization of DBP, HA-DEK, and HA-USF1 was visualized by IF analyses using
327 anti-DBP and anti-HA antibodies (Fig. 5C). In mock-infected cells, both HA-tagged
328 proteins showed nuclear localization, and in the case of HA-DEK, a strong signal was
329 observed at the nuclear periphery. At 18 hpi, HA-DEK appeared to be excluded from
330 VDRF (Fig. 5C, HA-DEK). However, in contrast to HA-DEK, we observed that
331 HA-USF1 could be localized inside VDRF (Fig. 5C, HA-USF1). Taken together, our
332 IF analyses suggest that VDRF may allow selective access of cellular nuclear proteins,
333 and at least one of transcription factors, USF1, is able to access the inside of VDRF.

334

335 **Oligomerization of DBP is critical for the histone exclusion from VDRF.**

336 To investigate the mechanism of the histone exclusion from VDRF, we
337 hypothesized that DBP may play a role, since an abundant amount of DBP is associated
338 with Ad DNA in VDRF. The crystal structure of DBP revealed that this protein has a
339 17 aa extension at its C-terminus (see Fig. 6A), and this C-terminal “arm” hooks onto
340 the next DBP molecule, resulting in oligomerization of DBP (47). It was also reported
341 that oligomerization of DBP mediated by the C-terminal “arm” enables
342 ATP-independent unwinding of dsDNA, and thus full-length DBP, but not the deletion
343 mutant that lacks the C-terminal “arm” (DBP Δ C), could support viral DNA replication
344 *in vitro* (9). Therefore, to examine a role of DBP and its oligomerization on the
345 histone localization, HeLa cells expressing histone H3.3-EGFP were transfected with

346 the expression vectors for HA-tagged full-length DBP or DBP Δ C and at 36 hpt
347 subjected to western blotting and IF assays using anti-HA and anti-DBP antibodies (Fig.
348 6B and C). The expression levels of both DBP proteins were almost the same as
349 indicated by western blotting (Fig. 6B). In IF analyses, we observed that full-length
350 DBP forms the foci like VDRF in the absence of any viral proteins/DNA, and histone
351 H3.3-EGFP was excluded from these foci as observed in infected cells (Fig. 6C,
352 HA-DBP). In sharp contrast, DBP Δ C was localized throughout the nucleus and did
353 not form such foci (Fig. 6C, HA-DBP Δ C). Taken together, these results suggest that
354 the oligomerization of DBP has a critical role in the histone exclusion from VDRF.

355

356

357 **DISCUSSION**

358 In this study we showed that replication-independent histone variant H3.3 is
359 deposited onto both incoming and newly synthesized Ad DNA (Fig. 3). These results,
360 together with the results from knockdown experiments of CAF-1 (Fig. 2) and
361 microscopic analyses (Figs. 4, 5, and 6), indicated that the histone deposition onto the
362 replicated virus genome is most likely uncoupled with viral DNA replication. Based
363 on these results, together with the previous our work (20), we hypothesize a model with
364 respect to the fluctuation of viral chromatin structure during infection cycle (Fig. 7).
365 In virions, viral DNA is tightly packed with viral core proteins (13). After the entry to
366 the cell, cellular histones are incorporated into incoming viral DNA-protein VII
367 complexes in the nucleus, and viral chromatin composed of both protein VII and
368 histones functions as template for viral early gene expression (20). In this process,
369 histone H3.3 is specifically deposited onto viral DNA, possibly by a histone chaperone
370 HIRA (34). As infection proceeds and then viral DNA replication is initiated,
371 oligomerization of DBP establishes the “histone-free” environment for viral DNA
372 replication. Newly synthesized viral DNA is then associated with histone H3.3 in a
373 replication-uncoupling fashion and might be acting as template for viral late gene
374 expression outside VDRF (31). In later phases of infection (24~ hpi), both histones
375 and newly synthesized core proteins VII and V are associated with viral DNA, which
376 likely reflects the processes during the progeny virion assembly (35). Since histones
377 are not included in virions, histones must be removed and replaced with newly
378 synthesized core proteins for progeny virions. Although the packaging mechanism of

379 progeny viral DNA during virion assembly remains unclear, we have reported the
380 involvement of a nucleolar protein B23/nucleophosmin in the regulation of viral
381 chromatin structure during progeny virion assembly (35, 36).

382 The mechanistic details of the histone deposition after viral DNA replication
383 remain still unclear. First, what factor(s) is involved in the histone deposition at late
384 phases of infection? HIRA is a potential candidate for this process, likewise in early
385 phases of infection (34). However, we did not perform knockdown experiments for
386 HIRA, since even if we could observe some effect of HIRA knockdown on viral
387 chromatin in late phases of infection, we could hardly distinguish whether the
388 knockdown directly affects the chromatin structure of progeny viral DNA or the effect
389 is derived indirectly from earlier events on incoming viral chromatin. IF analyses
390 showed that the localization of HIRA was not drastically changed during infection cycle
391 (Fig. 5A). Recent reports indicated that Daxx, a component of PML bodies, is also an
392 H3.3-specific histone chaperone (10, 21). However, Daxx seems not to function the
393 H3.3 deposition onto viral DNA because during Ad infection, some components of PML
394 bodies including Daxx are re-localized by viral protein E4orf3, possibly for inactivation
395 of the components (6, 42). Indeed, it is shown that Daxx-mediated antiviral response
396 is antagonized by E4orf3 (48). It is also revealed that Daxx negatively functions and
397 undergoes E1B-55K- and proteasome-dependent degradation during Ad infection (39).
398 Furthermore, most recently Schreiner *et al.* reported that during/immediately after
399 nuclear import of incoming virus genome, protein VI, one of capsid proteins, binds to
400 and counteracts Daxx, at least partly by displacing it from PML bodies (38). These

401 reports strongly suggest that Daxx is inactivated entirely throughout infection cycle by
402 viral proteins. DEK is also recently reported as a chaperone for histone H3.3 in
403 *Drosophila* cells (37), but it is unknown whether human DEK also functions as a
404 variant-specific chaperone or not. Our IF analyses indicated that exogenously
405 expressed DEK is excluded from VDRF (Fig. 5B and C). Further studies are needed
406 to elucidate the functions of these factors in late phases of infection.

407 In this study, we could not observe a role of CAF-1 in the histone deposition
408 onto viral DNA, while the accumulation of CAF-1 at VDRF was observed (Figs. 2 and
409 4A). CAF-1 knockdown did not affect the binding levels of histone H3 on viral
410 chromatin (Fig. 2C). Although we could not exclude the possibility that the
411 knockdown efficiency of CAF-1 is not sufficient in the condition employed here, we
412 concluded that the function of CAF-1 is largely inhibited under our condition: We
413 observed that siCAF-1-treated cells exhibit aberrant cell shapes (data not show) and the
414 knockdown affects viral gene expression (see below). Second, histone H3.3 is
415 selectively incorporated into viral chromatin (Fig. 3), while CAF-1 generally functions
416 as a chaperone for H3.1 and H3.2 (43). Third, although CAF-1 is reported to be able
417 to be associated with H3.3 under some specific conditions (10, 21), we could not
418 observe any interaction between CAF-1 and H3.3 during Ad infection, at least, in our
419 experimental conditions (data not shown). In addition to their roles during DNA
420 replication, CAF-1 and PCNA are also reported to be involved in the DNA damage
421 response pathway (29). Carson *et al.* reported that the DNA damage response pathway
422 is only partially activated during Ad infection, and some related factors, such as ATRIP

423 and TopBP1, are accumulated at VDRF (5). Therefore, CAF-1 (and PCNA) might
424 localize at VDRF in the course of this limited DNA damage response. Recently, it was
425 reported that FANCD2, one of factors involved in the DNA damage response, is
426 accumulated at VDRF, and loss of this protein results in less expression of viral late, but
427 not early, genes (8). Similarly, we observed that CAF-1 knockdown affects mRNA
428 levels of viral late genes without any effect on viral DNA replication (unpublished
429 observation). Thus, factors related to the DNA damage response such as FANCD2 and
430 CAF-1 might be required for viral late gene expression, although the underlying
431 mechanisms are unknown. In our condition, CAF-1 knockdown did not affect the
432 binding level of histone H3 on cellular chromatin (Fig. 2C, rDNA). This is consistent
433 with the report that loss of CAF-1 impairs replication-coupled deposition of histones but
434 the formation of nucleosome arrays on genomic DNA is still observed in the absence of
435 CAF-1 (44). In addition, a recent report demonstrated that a defect of histone H3.1
436 deposition by CAF-1 depletion could be rescued by HIRA-mediated H3.3 deposition
437 (33). Thus, in the case of cellular chromatin, alternative histone deposition pathway(s)
438 could rescue the loss of CAF-1 function.

439 It remains to be clarified what is the biological/virological significance of
440 histone deposition uncoupled with viral DNA replication. On cellular chromatin, a
441 replication-dependent histone chaperone CAF-1 is associated with the DNA replication
442 machinery and deposits histone H3.1-H4 (and H3.2-H4) complexes during DNA
443 replication (14, 40, 43). This DNA replication-coupled system of the histone
444 deposition is thought to be also utilized by some DNA viruses. For instance, DNA

445 replication of SV40 is largely depending on the cellular replication machinery, and
446 indeed CAF-1 was originally identified using *cell-free* DNA replication systems of
447 SV40 (41). In cytomegalovirus infection, it is reported that cellular histones, CAF-1,
448 and PCNA are accumulated at viral replication compartments (25). In the case of
449 herpes simplex virus type 1, it is shown that histone H3.3 is first deposited onto
450 incoming viral DNA by HIRA, and then H3.1 becomes associated with viral DNA
451 accompanied with viral DNA replication (28). It is suggested that this functional link
452 between DNA replication and the histone deposition enables to transfer “epigenetic
453 memory” such as histone modifications to the daughter DNA strands (43). Thus, some
454 DNA viruses might take advantage of this system for late gene expression, which
455 generally occurs after viral DNA replication. On the other hand, Ad seems to utilize
456 another strategy, that is, the uncoupling mechanism, as shown here. Like other DNA
457 viruses, Ad late genes are expressed only after the onset of viral DNA replication.
458 Thomas and Mathews demonstrated that Ad late gene expression requires its DNA
459 replication in *cis* (45), although the molecular mechanism remains to be determined.
460 This report leads us to hypothesize that the regulation of viral chromatin structure
461 during DNA replication could be an important process for the late gene expression. In
462 general, histone/nucleosome structure on DNA restricts the access of *trans*-acting
463 factors, such as transcription factors. In this view, DBP is an attractive candidate of the
464 key regulatory factor for DNA replication-dependent expression of viral late genes.
465 By oligomerization, DBP is able to not only support viral DNA replication, but also
466 establish the “histone-free” environment, which could be an opportunity window for

467 transcription factors to access the viral DNA for the activation of viral late genes. Our
468 IF analyses showed that transcription factor USF1, which binds to the MLP region after
469 viral DNA replication (46), are not excluded from VDRF (Fig. 5B and C), supporting
470 this notion. Further, this is in agreement with the report that DBP enhances the
471 binding of USF1 to the MLP region *in vitro* (51). Overall, we speculate that
472 uncoupling of the histone deposition with viral DNA replication is mediated by DBP
473 oligomerization, at least partly, and plays a role in DNA replication-dependent
474 activation of viral late gene expression.

475 The expression of certain cellular genes, such as *HoxB* gene, is shown to
476 require DNA replication (12). However, the regulation mechanism of “DNA
477 replication-dependent gene expression” remains to be determined. As Ad has late
478 genes, the expression of which are DNA replication-dependent (45), this virus could be
479 a good model for the analyses of such regulations. Therefore, this study might give a
480 clue for understanding the functional relationship between DNA replication and
481 transcription on cellular and/or viral chromatin.

482

483 **ACKNOWLEDGMENTS**

484 We thank Drs. M. Okuwaki, S. Saito, A. Verreault, and W. C. Russel, and K.
485 Kajitani for their kind gifts. This work was supported in part by Grants-in-aid for
486 Scientific Research from the Ministry of Education, Culture, Sports, Science and
487 Technology of Japan (to K.N.) and the University of Tsukuba Research Infrastructure
488 Support Program (to T.K.).
489

490 **REFERECES**

- 491 1. **Ahmad, K., and S. Henikoff.** 2002. The histone variant H3.3 marks active
492 chromatin by replication-independent nucleosome assembly. *Mol Cell*
493 **9**:1191-200.
- 494 2. **Bell, O., V. K. Tiwari, N. H. Thoma, and D. Schubeler.** 2011. Determinants
495 and dynamics of genome accessibility. *Nat Rev Genet* **12**:554-64.
- 496 3. **Beyer, A. L., A. H. Bouton, L. D. Hodge, and O. L. Miller, Jr.** 1981.
497 Visualization of the major late R strand transcription unit of adenovirus serotype
498 2. *J Mol Biol* **147**:269-95.
- 499 4. **Burg, J. L., J. Schweitzer, and E. Daniell.** 1983. Introduction of superhelical
500 turns into DNA by adenoviral core proteins and chromatin assembly factors. *J*
501 *Virol* **46**:749-55.
- 502 5. **Carson, C. T., N. I. Orazio, D. V. Lee, J. Suh, S. Bekker-Jensen, F. D. Araujo,**
503 **S. S. Lakdawala, C. E. Lilley, J. Bartek, J. Lukas, and M. D. Weitzman.**
504 2009. Mislocalization of the MRN complex prevents ATR signaling during
505 adenovirus infection. *EMBO J* **28**:652-62.
- 506 6. **Carvalho, T., J. S. Seeler, K. Ohman, P. Jordan, U. Pettersson, G. Akusjarvi,**
507 **M. Carmo-Fonseca, and A. Dejean.** 1995. Targeting of adenovirus E1A and
508 E4-ORF3 proteins to nuclear matrix-associated PML bodies. *J Cell Biol*
509 **131**:45-56.
- 510 7. **Chatterjee, P. K., M. E. Vayda, and S. J. Flint.** 1986. Adenoviral protein VII
511 packages intracellular viral DNA throughout the early phase of infection. *EMBO*
512 *J* **5**:1633-44.
- 513 8. **Cherubini, G., V. Naim, P. Caruso, R. Burla, M. Bogliolo, E. Cundari, K.**
514 **Benihoud, I. Saggio, and F. Rosselli.** 2011. The FANC pathway is activated by
515 adenovirus infection and promotes viral replication-dependent recombination.
516 *Nucleic Acids Res* **39**:5459-73.
- 517 9. **Dekker, J., P. N. Kanellopoulos, A. K. Loonstra, J. A. van Oosterhout, K.**
518 **Leonard, P. A. Tucker, and P. C. van der Vliet.** 1997. Multimerization of the
519 adenovirus DNA-binding protein is the driving force for ATP-independent DNA
520 unwinding during strand displacement synthesis. *EMBO J* **16**:1455-63.
- 521 10. **Drane, P., K. Ouararhni, A. Depaux, M. Shuaib, and A. Hamiche.** 2010. The

- 522 death-associated protein DAXX is a novel histone chaperone involved in the
523 replication-independent deposition of H3.3. *Genes Dev* **24**:1253-65.
- 524 11. **Elsaesser, S. J., A. D. Goldberg, and C. D. Allis.** 2010. New functions for an
525 old variant: no substitute for histone H3.3. *Curr Opin Genet Dev* **20**:110-7.
- 526 12. **Fisher, D., and M. Mechali.** 2003. Vertebrate HoxB gene expression requires
527 DNA replication. *EMBO J* **22**:3737-48.
- 528 13. **Giberson, A. N., A. R. Davidson, and R. J. Parks.** 2011. Chromatin structure
529 of adenovirus DNA throughout infection. *Nucleic Acids Res* (in press). doi:
530 10.1093/nar/gkr1076.
- 531 14. **Groth, A., W. Rocha, A. Verreault, and G. Almouzni.** 2007. Chromatin
532 challenges during DNA replication and repair. *Cell* **128**:721-33.
- 533 15. **Gyurcsik, B., H. Haruki, T. Takahashi, H. Mihara, and K. Nagata.** 2006.
534 Binding modes of the precursor of adenovirus major core protein VII to DNA
535 and template activating factor I: implication for the mechanism of remodeling of
536 the adenovirus chromatin. *Biochemistry* **45**:303-13.
- 537 16. **Hake, S. B., and C. D. Allis.** 2006. Histone H3 variants and their potential role
538 in indexing mammalian genomes: the "H3 barcode hypothesis". *Proc Natl Acad*
539 *Sci U S A* **103**:6428-35.
- 540 17. **Haruki, H., B. Gyurcsik, M. Okuwaki, and K. Nagata.** 2003. Ternary
541 complex formation between DNA-adenovirus core protein VII and
542 TAF-Ibeta/SET, an acidic molecular chaperone. *FEBS Lett* **555**:521-7.
- 543 18. **Haruki, H., M. Okuwaki, M. Miyagishi, K. Taira, and K. Nagata.** 2006.
544 Involvement of template-activating factor I/SET in transcription of adenovirus
545 early genes as a positive-acting factor. *J Virol* **80**:794-801.
- 546 19. **Kawase, H., M. Okuwaki, M. Miyaji, R. Ohba, H. Handa, Y. Ishimi, T.**
547 **Fujii-Nakata, A. Kikuchi, and K. Nagata.** 1996. NAP-I is a functional
548 homologue of TAF-I that is required for replication and transcription of the
549 adenovirus genome in a chromatin-like structure. *Genes Cells* **1**:1045-56.
- 550 20. **Komatsu, T., H. Haruki, and K. Nagata.** 2011. Cellular and viral chromatin
551 proteins are positive factors in the regulation of adenovirus gene expression.
552 *Nucleic Acids Res* **39**:889-901.
- 553 21. **Lewis, P. W., S. J. Elsaesser, K. M. Noh, S. C. Stadler, and C. D. Allis.** 2010.
554 Daxx is an H3.3-specific histone chaperone and cooperates with ATRX in

- 555 replication-independent chromatin assembly at telomeres. Proc Natl Acad Sci U
556 S A **107**:14075-80.
- 557 22. **Matsumoto, K., K. Nagata, M. Ui, and F. Hanaoka.** 1993. Template activating
558 factor I, a novel host factor required to stimulate the adenovirus core DNA
559 replication. J Biol Chem **268**:10582-7.
- 560 23. **Matsumoto, K., M. Okuwaki, H. Kawase, H. Handa, F. Hanaoka, and K.**
561 **Nagata.** 1995. Stimulation of DNA transcription by the replication factor from
562 the adenovirus genome in a chromatin-like structure. J Biol Chem **270**:9645-50.
- 563 24. **Nagata, K., H. Kawase, H. Handa, K. Yano, M. Yamasaki, Y. Ishimi, A.**
564 **Okuda, A. Kikuchi, and K. Matsumoto.** 1995. Replication factor encoded by a
565 putative oncogene, set, associated with myeloid leukemogenesis. Proc Natl Acad
566 Sci U S A **92**:4279-83.
- 567 25. **Nitzsche, A., C. Paulus, and M. Nevels.** 2008. Temporal dynamics of
568 cytomegalovirus chromatin assembly in productively infected human cells. J
569 Virol **82**:11167-80.
- 570 26. **Okuwaki, M., A. Iwamatsu, M. Tsujimoto, and K. Nagata.** 2001.
571 Identification of nucleophosmin/B23, an acidic nucleolar protein, as a
572 stimulatory factor for in vitro replication of adenovirus DNA complexed with
573 viral basic core proteins. J Mol Biol **311**:41-55.
- 574 27. **Okuwaki, M., and K. Nagata.** 1998. Template activating factor-I remodels the
575 chromatin structure and stimulates transcription from the chromatin template. J
576 Biol Chem **273**:34511-8.
- 577 28. **Placek, B. J., J. Huang, J. R. Kent, J. Dorsey, L. Rice, N. W. Fraser, and S.**
578 **L. Berger.** 2009. The histone variant H3.3 regulates gene expression during lytic
579 infection with herpes simplex virus type 1. J Virol **83**:1416-21.
- 580 29. **Polo, S. E., D. Roche, and G. Almouzni.** 2006. New histone incorporation
581 marks sites of UV repair in human cells. Cell **127**:481-93.
- 582 30. **Polo, S. E., S. E. Theocharis, J. Klijanienko, A. Savignoni, B. Asselain, P.**
583 **Vielh, and G. Almouzni.** 2004. Chromatin assembly factor-1, a marker of
584 clinical value to distinguish quiescent from proliferating cells. Cancer Res
585 **64**:2371-81.
- 586 31. **Pombo, A., J. Ferreira, E. Bridge, and M. Carmo-Fonseca.** 1994. Adenovirus
587 replication and transcription sites are spatially separated in the nucleus of

- 588 infected cells. *EMBO J* **13**:5075-85.
- 589 32. **Ray-Gallet, D., J. P. Quivy, C. Scamps, E. M. Martini, M. Lipinski, and G.**
590 **Almouzni.** 2002. HIRA is critical for a nucleosome assembly pathway
591 independent of DNA synthesis. *Mol Cell* **9**:1091-100.
- 592 33. **Ray-Gallet, D., A. Woolfe, I. Vassias, C. Pellentz, N. Lacoste, A. Puri, D. C.**
593 **Schultz, N. A. Pchelintsev, P. D. Adams, L. E. Jansen, and G. Almouzni.** 2011.
594 Dynamics of histone h3 deposition in vivo reveal a nucleosome gap-filling
595 mechanism for h3.3 to maintain chromatin integrity. *Mol Cell* **44**:928-41.
- 596 34. **Ross, P. J., M. A. Kennedy, C. Christou, M. Risco Quiroz, K. L. Poulin, and**
597 **R. J. Parks.** 2011. Assembly of helper-dependent adenovirus DNA into
598 chromatin promotes efficient gene expression. *J Virol* **85**:3950-8.
- 599 35. **Samad, M. A., T. Komatsu, M. Okuwaki, and K. Nagata.** 2012.
600 B23/Nucleophosmin is involved in regulation of adenovirus chromatin structure
601 at late infection stages, but not in its replication and transcription. *J Gen Virol*
602 (in press). doi: 10.1099/vir.0.036665-0.
- 603 36. **Samad, M. A., M. Okuwaki, H. Haruki, and K. Nagata.** 2007. Physical and
604 functional interaction between a nucleolar protein nucleophosmin/B23 and
605 adenovirus basic core proteins. *FEBS Lett* **581**:3283-8.
- 606 37. **Sawatsubashi, S., T. Murata, J. Lim, R. Fujiki, S. Ito, E. Suzuki, M. Tanabe,**
607 **Y. Zhao, S. Kimura, S. Fujiyama, T. Ueda, D. Umetsu, T. Ito, K. Takeyama,**
608 **and S. Kato.** 2010. A histone chaperone, DEK, transcriptionally coactivates a
609 nuclear receptor. *Genes Dev* **24**:159-70.
- 610 38. **Schreiner, S., R. Martinez, P. Groitl, F. Rayne, R. Vaillant, P. Wimmer, G.**
611 **Bossis, T. Sternsdorf, L. Marcinowski, Z. Ruzsics, T. Dobner, and H.**
612 **Wodrich.** 2012. Transcriptional Activation of the Adenoviral Genome Is
613 Mediated by Capsid Protein VI. *PLoS Pathog* **8**:e1002549.
- 614 39. **Schreiner, S., P. Wimmer, H. Sirma, R. D. Everett, P. Blanchette, P. Groitl,**
615 **and T. Dobner.** 2010. Proteasome-dependent degradation of Daxx by the viral
616 E1B-55K protein in human adenovirus-infected cells. *J Virol* **84**:7029-38.
- 617 40. **Shibahara, K., and B. Stillman.** 1999. Replication-dependent marking of DNA
618 by PCNA facilitates CAF-1-coupled inheritance of chromatin. *Cell* **96**:575-85.
- 619 41. **Smith, S., and B. Stillman.** 1989. Purification and characterization of CAF-I, a
620 human cell factor required for chromatin assembly during DNA replication in

- 621 vitro. *Cell* **58**:15-25.
- 622 42. **Stracker, T. H., D. V. Lee, C. T. Carson, F. D. Araujo, D. A. Ornelles, and M.**
623 **D. Weitzman.** 2005. Serotype-specific reorganization of the Mre11 complex by
624 adenoviral E4orf3 proteins. *J Virol* **79**:6664-73.
- 625 43. **Tagami, H., D. Ray-Gallet, G. Almouzni, and Y. Nakatani.** 2004. Histone
626 H3.1 and H3.3 complexes mediate nucleosome assembly pathways dependent or
627 independent of DNA synthesis. *Cell* **116**:51-61.
- 628 44. **Takami, Y., T. Ono, T. Fukagawa, K. Shibahara, and T. Nakayama.** 2007.
629 Essential role of chromatin assembly factor-1-mediated rapid nucleosome
630 assembly for DNA replication and cell division in vertebrate cells. *Mol Biol Cell*
631 **18**:129-41.
- 632 45. **Thomas, G. P., and M. B. Mathews.** 1980. DNA replication and the early to
633 late transition in adenovirus infection. *Cell* **22**:523-33.
- 634 46. **Toth, M., W. Doerfler, and T. Shenk.** 1992. Adenovirus DNA replication
635 facilitates binding of the MLTF/USF transcription factor to the viral major late
636 promoter within infected cells. *Nucleic Acids Res* **20**:5143-8.
- 637 47. **Tucker, P. A., D. Tsernoglou, A. D. Tucker, F. E. Coenjaerts, H. Leenders,**
638 **and P. C. van der Vliet.** 1994. Crystal structure of the adenovirus DNA binding
639 protein reveals a hook-on model for cooperative DNA binding. *EMBO J*
640 **13**:2994-3002.
- 641 48. **Ullman, A. J., and P. Hearing.** 2008. Cellular proteins PML and Daxx mediate
642 an innate antiviral defense antagonized by the adenovirus E4 ORF3 protein. *J*
643 *Virol* **82**:7325-35.
- 644 49. **Vayda, M. E., A. E. Rogers, and S. J. Flint.** 1983. The structure of
645 nucleoprotein cores released from adenovirions. *Nucleic Acids Res* **11**:441-60.
- 646 50. **Verreault, A., P. D. Kaufman, R. Kobayashi, and B. Stillman.** 1996.
647 Nucleosome assembly by a complex of CAF-1 and acetylated histones H3/H4.
648 *Cell* **87**:95-104.
- 649 51. **Zijderveld, D. C., F. d'Adda di Fagagna, M. Giacca, H. T. Timmers, and P.**
650 **C. van der Vliet.** 1994. Stimulation of the adenovirus major late promoter in
651 vitro by transcription factor USF is enhanced by the adenovirus DNA binding
652 protein. *J Virol* **68**:8288-95.
- 653

654

655

656 **FIGURE LEGENDS**

657 **FIG. 1. Viral chromatin structure in early and late phases of infection.** (A)

658 The structure of Ad genome. Arrows represent promoters of viral genes. Target

659 regions for ChIP assays are indicated by arrowheads. (B) The amounts of viral DNA.

660 HeLa cells were infected with HAdV5 at an MOI of 100, and DNA samples were

661 purified from infected cells at 6 and 12 hpi. The amount of viral DNA was

662 quantitatively measured by qPCR using primers for the E1A promoter region. The

663 amount of viral DNA was graphed as the ratio relative to that at 6 hpi. (C) ChIP

664 assays. HeLa cells were infected with HAdV5 at an MOI of 100 and subjected to

665 ChIP assays using infected cells at 6 and 12 hpi. Immunoprecipitation was carried out

666 using indicated antibodies and anti-FLAG antibody (as a negative control). The

667 obtained DNAs were quantitatively measured by qPCR using indicated primer sets.

668 The binding levels of each protein were calculated as relative enrichment against that

669 obtained in a negative control (anti-FLAG antibody). (D) The binding levels of core

670 histones. Base on the results of ChIP assays shown in (C), the binding level of histone

671 H4 and H2A-H2B was normalized by that of histone H3.

672

673 **FIG. 2. Localization and role of PCNA and CAF-1 during viral DNA replication.**

674 (A) IF assays. HeLa cells and cells stably expressing HA-PCNA grown on cover

675 slips were mock-infected or infected with HAdV5 at an MOI of 50. At 18 hpi the

676 localization patterns of HA-PCNA and DBP were analyzed by IF using anti-HA and

677 anti-DBP antibodies. DNA was visualized by TO-PRO-3 iodide staining. Merged

678 images are also indicated. Higher-magnified images of the regions marked by squares
679 are shown below. (B) RT-qPCR assays. HeLa cells were treated with siControl or
680 siCAF-1 and then either mock-infected or infected with HAdV5 at an MOI of 100, and
681 total RNAs were purified at 6 and 12 hpi. cDNAs were synthesized with reverse
682 transcription and subjected to qPCR using primer sets for *CAF-1 p150* and *GAPDH*
683 mRNAs. The mRNA levels relative to those in control cells at 12 hpi were graphed.
684 (C) ChIP assays. siRNA-treated cells were infected with HAdV5 at an MOI of 100
685 and at 6 and 12 hpi subjected to ChIP assays using anti-histone H3 and anti-FLAG
686 antibodies as described above. (D) Relative amounts of viral DNA. Viral DNA
687 was purified from lysates for ChIP assays in (C) and subjected to qPCR using primer set
688 for the E1A promoter. The DNA amounts at 12 hpi relative to those at 6 hpi were
689 shown.

690

691 **FIG. 3. Incorporation of histone H3 variants into viral chromatin.** (A, B) ChIP
692 assays with FLAG-tagged histone H3 variants. HeLa cells were transfected with
693 pcDNA3 empty vector, pcDNA3-H3.2-FLAG, or pcDNA3-H3.3-FLAG, and at 24 hpt
694 (hours post transfection) infected with HAdV5 at an MOI of 100. At 2, 6, and 10 hpi
695 (A) or 12 hpi (B), ChIP assays were carried out using anti-FLAG and anti-HA (as a
696 negative control) antibodies, as described above. Note that in the case of 10 hpi, HU
697 was added to block viral DNA replication. The results were graphed as relative
698 enrichment as described above. (C) Western blot analyses. At 24 hpt, lysates were
699 prepared from cells transfected with pcDNA3 empty (lane 1), pcDNA3-H3.2-FLAG

700 (lane 2), and pcDNA3-H3.3-FLAG (lane 3) and subjected to 15% SDS-PAGE, followed
701 by western blot analyses using anti-FLAG (upper panel) and anti- β -actin (lower panel)
702 antibodies. (D) Western blot analyses. HeLa cells were transfected with pcDNA3
703 empty vector (lane 1), pcDNA3-H3.1-FLAG (Lane 2), or pcDNA3-H3.3-FLAG (lane 3),
704 and at 24 hpt lysates were prepared and subjected to 15% SDS-PAGE, followed by
705 western blot analyses using anti-FLAG (upper panel) and anti- β -actin (lower panel)
706 antibodies. (E) ChIP assays. HeLa cells transfected with pcDNA3 empty vector
707 (lanes 2, 3, 9, and 10), pcDNA3-H3.1-FLAG (lanes 4, 5, 11, and 12), or
708 pcDNA3-H3.3-FLAG (lanes 6, 7, 13, and 14) were infected with HA Δ V5 at an MOI of
709 100. At 10 hpi (left panels, lanes 1-7) or 12 hpi (right panels, lanes 8-14), ChIP assays
710 were carried out using anti-FLAG (lanes 3, 5, 7, 10, 12, and 14) and anti-HA (as a
711 negative control, lanes 2, 4, 6, 9, 11, and 13) antibodies. In the case of 10 hpi, HU was
712 added to block viral DNA replication. The immunoprecipitated DNAs were amplified
713 by semi-quantitative PCR using the indicated primer sets. PCR products were
714 separated on a 7% polyacrylamide gel and visualized by staining with EtBr. Input
715 DNAs (lanes 1 and 8) were purified from 0.5% of lysates of cells transfected with the
716 empty vector.

717

718 **FIG. 4. Localization of histones in late phases of infection.** (A) IF analyses
719 using cells stably expressing histone H3.3-EGFP. HeLa cells stably expressing histone
720 H3.3-EGFP grown on cover slips were mock-infected or infected at an MOI of 50, and
721 at 18 hpi subjected to IF assays using anti-DBP (upper panels) and anti-CAF-1 p150

722 (lower panels) antibodies, as described above. Higher-magnified images of the regions
723 marked by squares are shown below. (B) Localization of histone H3.2 in late phases
724 of infection. HeLa cells stably expressing histone H3.2-EGFP were mock-infected or
725 infected with HAdV5 at an MOI of 50, and at 18 hpi subjected to IF analyses using
726 anti-DBP antibody. Higher-magnified images of the regions marked by squares are
727 shown. (C) Localization of endogenous histone H2A in late phases of infection.
728 HeLa cells were mock-infected or infected with HAdV5 at an MOI of 50, and at 18 hpi
729 subjected to IF assays using anti-histone H2A and anti-DBP antibodies.
730 Higher-magnified images of the regions marked by squares are shown below. (D)
731 Histone localization in early phases of infection. HeLa cells stably expressing histone
732 H3.2-EGFP and H3.3-EGFP were mock-infected or infected with HAdV5 at an MOI of
733 250, and at 4 hpi subjected to IF analyses using anti-protein VII antibody.

734

735 **FIG. 5. Localization of nuclear proteins in late phases of infection.** (A) IF
736 analyses using anti-HIRA antibody. HeLa cells were mock-infected or infected with
737 HAdV5 at an MOI of 250 (for 4 hpi) or 50 (for 18 hpi) and subjected to IF analyses
738 using anti-protein VII and anti-HIRA antibodies. (B) Western blot analyses.
739 Lysates were prepared from HeLa cells transfected with pCHA-puro empty vector (lane
740 1), pCHA-DEK (Lane 2), or pCHA-puro-USF1 (lane 3) at 24 hpt, and subjected to 10%
741 SDS-PAGE, followed by western blot analyses using anti-HA (upper panel) and
742 anti- β -actin (lower panel) antibodies. (C) Localization of HA-DEK and HA-USF1.
743 HeLa cells were transfected pCHA-puro empty vector, pCHA-DEK, or

744 pCHA-puro-USF1. At 24 hpt, cells were mock-infected or infected with HAdV5 at an
745 MOI of 50, and at 18 hpi subjected to IF assays using anti-HA and anti-DBP antibodies.

746

747 **FIG. 6. Role of DBP oligomerization on histone localization.** (A) Schematic
748 diagrams of full-length DBP and C-terminally deleted mutant DBP Δ C. DBP of
749 HAdV5 consists of 529 aa, and the C-terminal 17 aa (513-529) functions as an “arm”
750 for oligomerization. DBP Δ C lacks the C-terminal 17 aa. (B) Western blot analyses.
751 HeLa cells stably expressing histone H3.3-EGFP were transfected with pCHA-puro
752 empty vector (lane 1), pCHA-puro-DBP (lane 2), or pCHA-puro-DBP Δ C (lane 3), and
753 lysates prepared at 36 hpt were subjected to 10% SDS-PAGE, followed by western blot
754 analyses using anti-HA (top), anti-DBP (middle), and anti- β -actin (bottom panel)
755 antibodies. (C) IF analyses. At 36 hpt, cells as described in (B) grown on cover
756 slips were subjected to IF analyses using anti-HA (left panels) and anti-DBP (right
757 panels) antibodies as described above. Higher-magnified images of the regions
758 marked by squares are shown below.

759

760 **FIG. 7. A hypothetical model for viral chromatin structure during infection cycle.**

761 For detail, see Discussion section.

762

Figure 1 Komatsu *et al.*

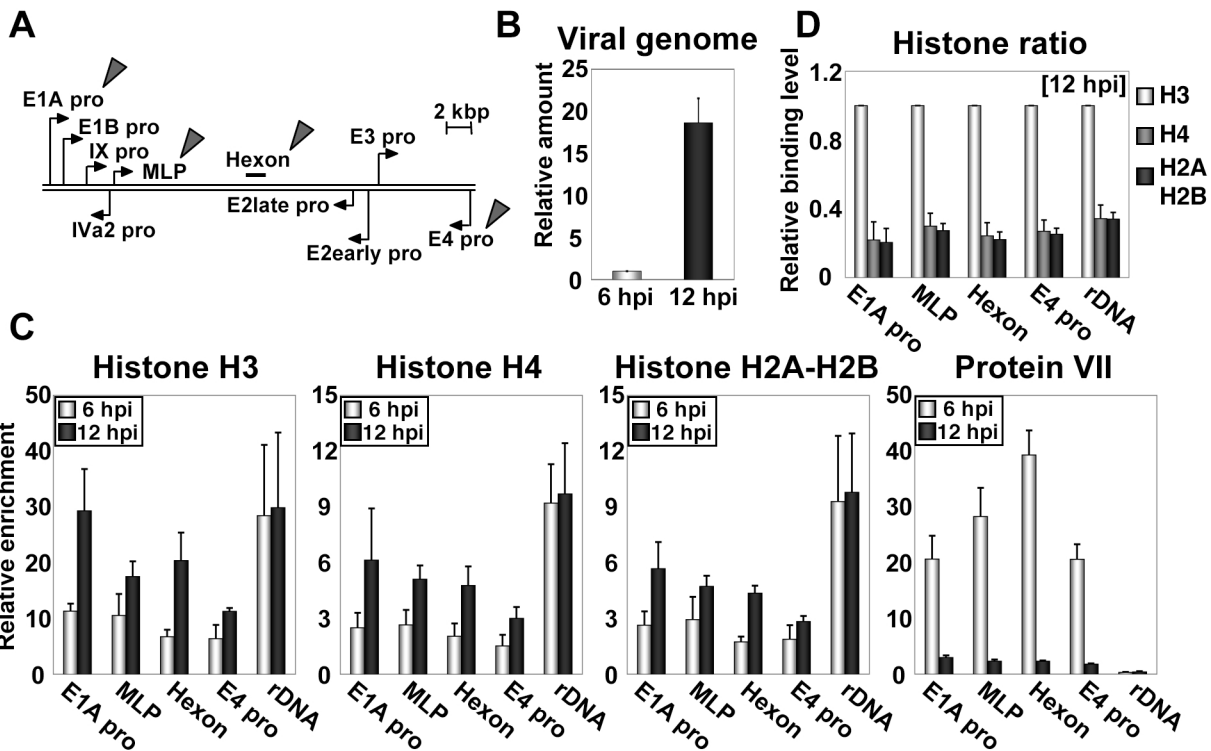
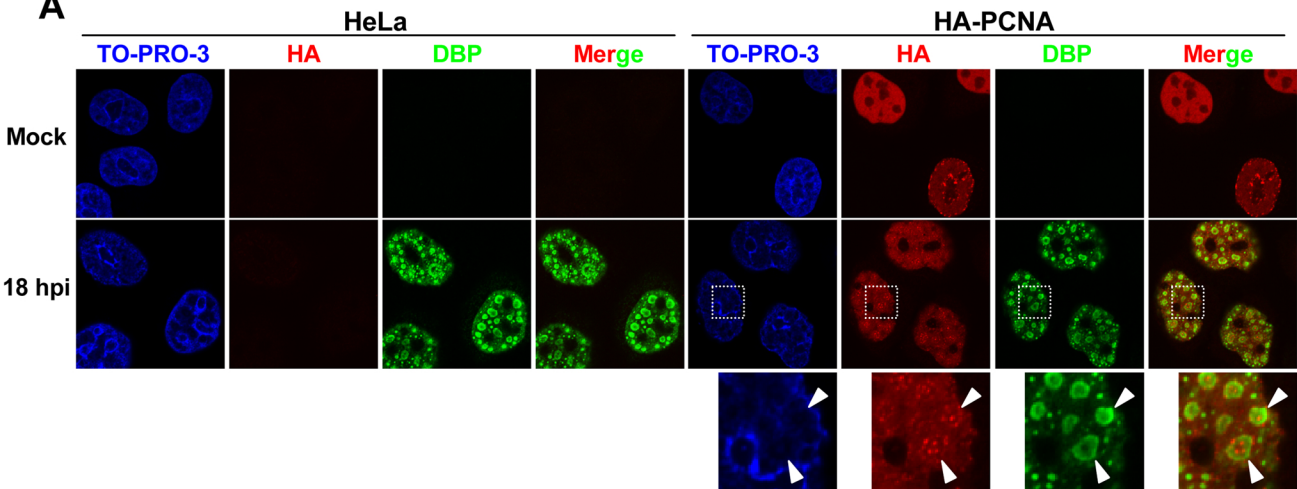
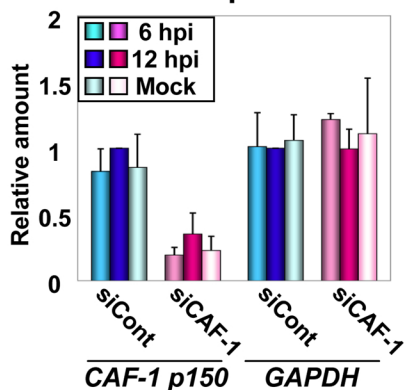


Figure 2 Komatsu *et al.*

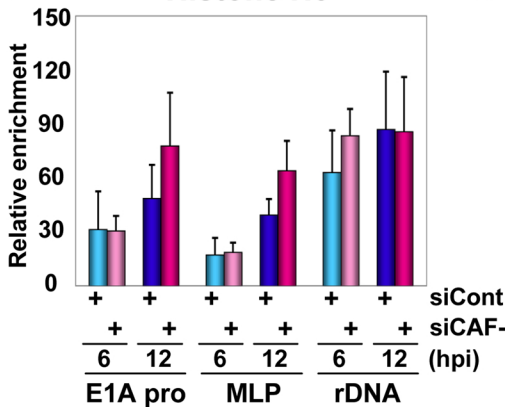
A



B RT-qPCR



C Histone H3



D Viral genome

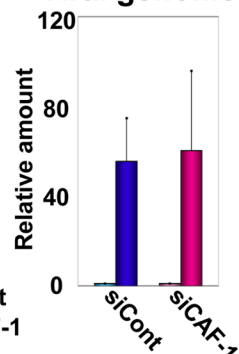


Figure 3 *Komatsu et al.*

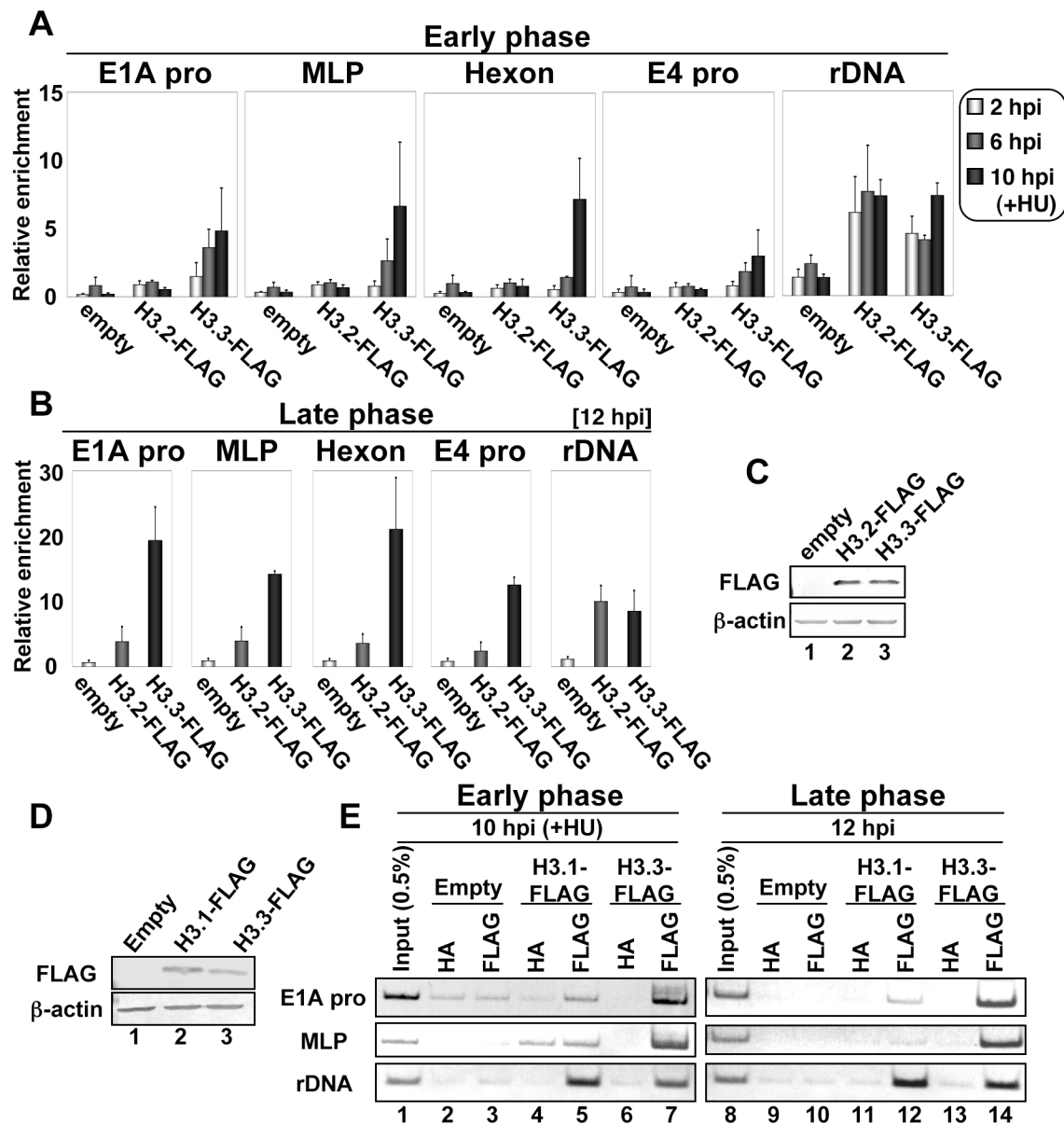


Figure 4 *Komatsu et al.*

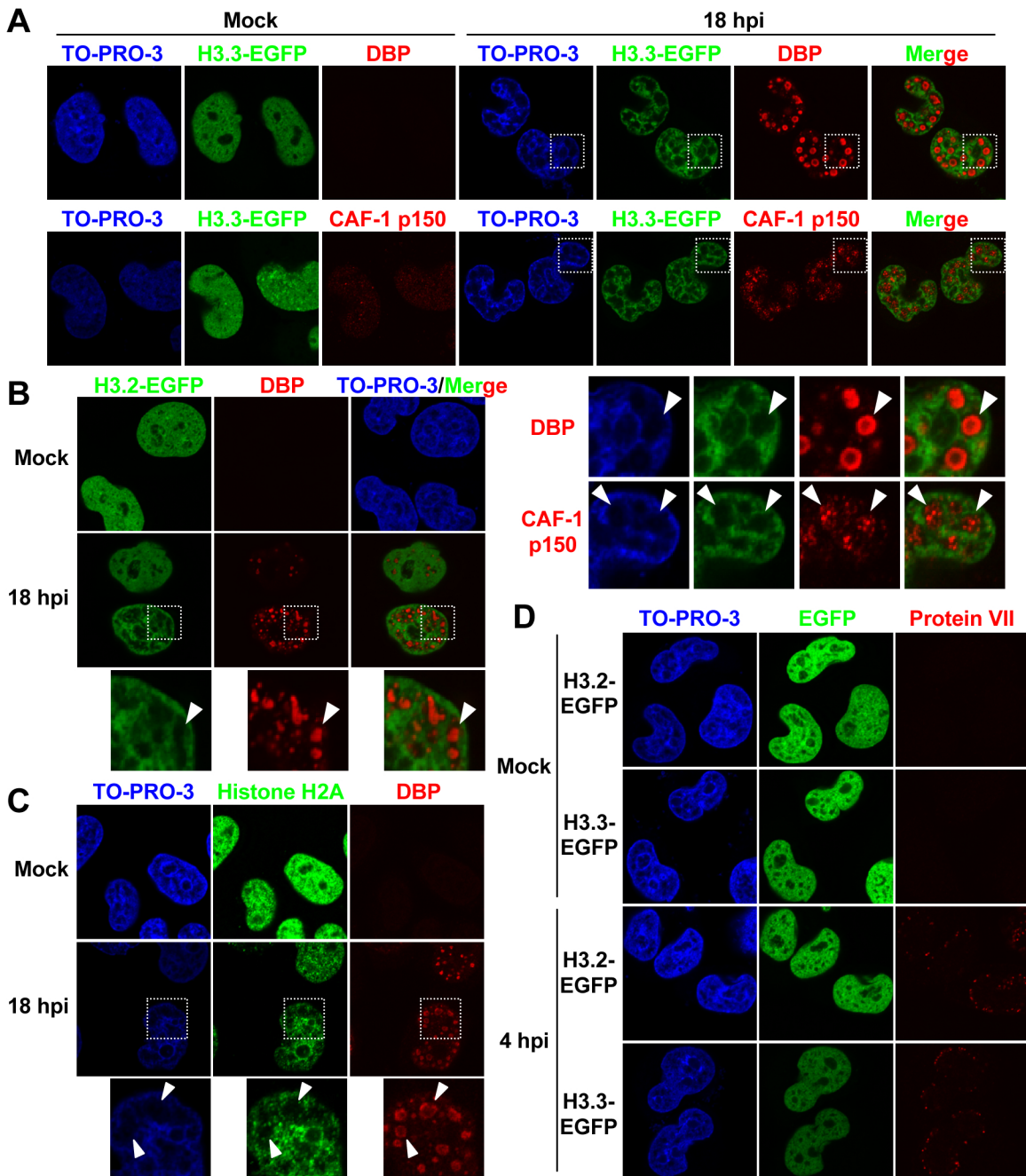


Figure 5 *Komatsu et al.*

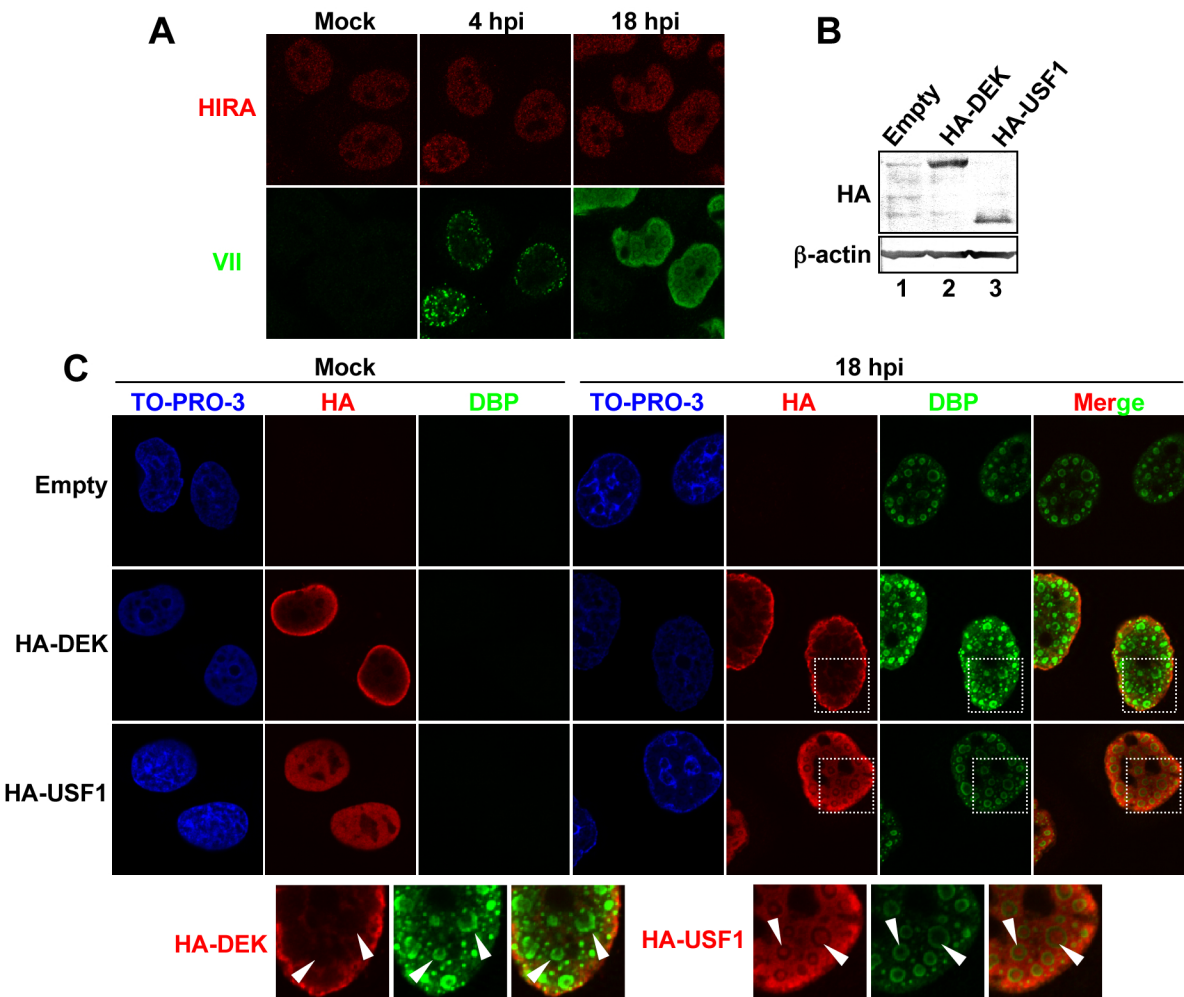


Figure 6 Komatsu *et al.*

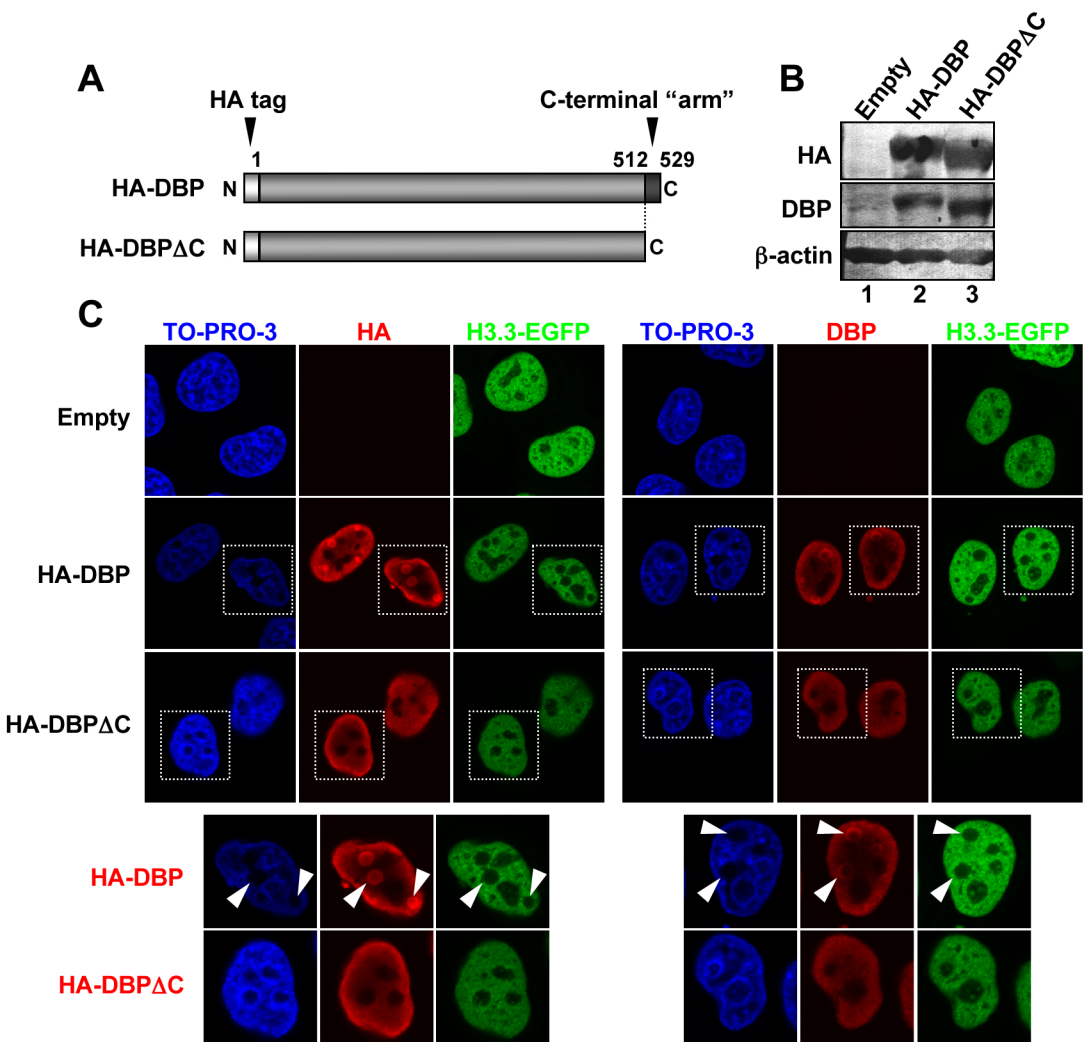
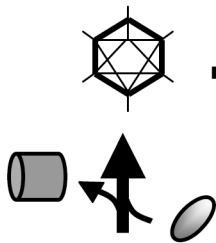


Figure 7 Komatsu *et al.*

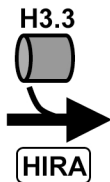
i) Virion



ii) Entry of nucleus



"VII" chromatin



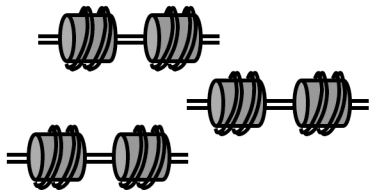
iii) Early phases



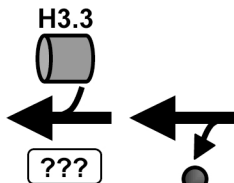
"Chimeric" chromatin



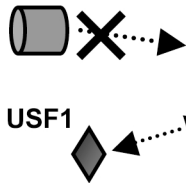
v) Late phases



"Nucleosomal" chromatin



iv) DNA replication



"Histone-free" replication foci formed by DBP oligomerization

